3D Localization, Mapping and Path Planning for Search and Rescue Operations

Author(s):
Dubé, Renaud; Gawel, Abel; Cadena, César; Siegwart, Roland; Freda, Luigi; Gianni, Mario

Publication date:
2016

Permanent link:
https://doi.org/10.3929/ethz-a-010819655

Originally published in:
https://doi.org/10.1109/SSRR.2016.7784311

3D Localization, Mapping and Path Planning for Search and Rescue Operations

R. Dubé*, A. Gawel*, C. Cadena, R. Siegwart
Autonomous Systems Lab - ETH Zurich, Switzerland

L. Freda*, M. Gianni
ALCOR Lab, DIAG - Sapienza University of Rome, Italy

***Abstract*—This work presents our results on 3D robot localization, mapping and path planning for the latest joint exercise of the European project "Long-Term Human-Robot Teaming for Robots Assisted Disaster Response" (TRADR)[1]. The full system is operated and evaluated by firemen end-users in real-world search and rescue experiments. We demonstrate that the system is able to plan a path to a goal position desired by the fireman operator in the TRADR Operational Control Unit (OCU), using a persistent 3D map created by the robot during previous sorties.**

I. INTRODUCTION

Teams of autonomous mobile robots have the potential to reduce human risks during disaster response as well as the associated costs [1]. Different levels of robot autonomy are required in order to effectively support a rescue squad performing high-level tasks such as exploring the disaster area, detecting victims and taking chemical samples. Moreover, long-term operation of robotic platforms is desired for humans and robots to collaborate over several days of disaster intervention. To this end, building and maintaining a persistent representation of the environment, accurate localization, and efficient path planning are fundamental prerequisites.

Prior to this work, a SLAM strategy based on Iterative Closest Point (ICP) for the robotic platform considered in this work was proposed in [2]. While providing precise local reconstruction of an environment, this technique can not improve the map in the event of place recognition. The localization algorithm presented in this paper is therefore based on the pose-graph SLAM strategy as described in [3].

The 3D path planning and navigation methods presented in this paper are based on the works [4, 5, 6]. The underlying modules provide functionalities such as real-time point cloud segmentation and traversability analysis. A randomized A* approach is applied on the current terrain structure interpretation.

In the remainder of this report, we concisely describe the localization, mapping and path planning systems and present the results of experiments with firemen end-users, at the latest TRADR Joint Exercise (TJEx).

II. SYSTEM DESCRIPTION

While the TRADR system comprises an integrated framework spanning from low-level perception functionalities to high-level reasoning, in this work we focus on presenting the latest advances in the integrated SLAM and path planning.

*R. Dubé, A. Gawel and L. Freda contributed equally to this work.

[1]This research is supported by EU-FP7-ICT-Project TRADR 609763. http://www.tradr-project.eu/

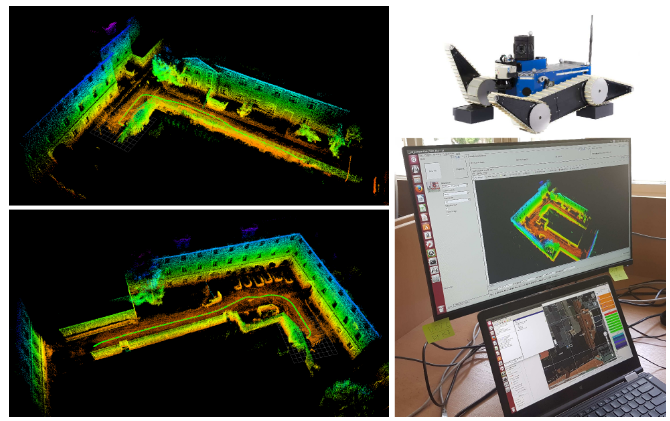

Figure 1: *Top-left*: 3D laser map generated in a first sortie on mission day 1. *Bottom-left*: Map generated during a second sortie on mission day 2. *Top-right*: TRADR UGV equipped with multiple encoders, an IMU and a rotating laser-scanner. *Bottom-right*: TRADR OCU displaying the merged map.

A. Pose-graph based localization, mapping and map merging

The proposed SLAM system relies on a pose-graph optimization approach [3]. This framework computes a Maximum A Posteriori (MAP) estimate of a trajectory of robot poses $\boldsymbol{c}(t_i) \in SE(3)$ collected at times $\{t_i\}_{i=0}^N$ by optimizing a negative log-posterior E (aka error function) which sums over constraints $\boldsymbol{\Theta}(\boldsymbol{c}_{i,j}) = \boldsymbol{e}_{i,j}^T \boldsymbol{\Omega}_{i,j} \boldsymbol{e}_{i,j}$, with $\boldsymbol{e}_{i,j} = \boldsymbol{z}_{i,j} - \tilde{\boldsymbol{z}}_{i,j}(\boldsymbol{c}_{i,j})$, and $\boldsymbol{z}_{i,j}$ the observation, $\tilde{\boldsymbol{z}}_{i,j}(\boldsymbol{c}_{i,j})$ the prediction and $\boldsymbol{\Omega}_{i,j}$ the information matrix. In the present system the function E is obtained by combining together *(i)* odometry constraints $\boldsymbol{\Theta}_O(\boldsymbol{c}_{i,j})$, fusing wheel encoders and IMU data along the lines of [7], and *(ii)* laser scan-matching constraints $\boldsymbol{\Theta}_S(\boldsymbol{c}_{i,j})$, from ICP matching the current scan against all previous scans within a sliding time window $[t-w, t] \subset \mathbb{R}$ where t is the current time and w is the chosen fixed time width. Let $\boldsymbol{c}(t_1{:}t_2)$ denote the sequence of robot poses acquired in the time interval $[t_1, t_2] \subset \mathbb{R}$ and $\mathcal{C}_O$ and $\mathcal{C}_S$ respectively the set of pairs of timestamps for which odometry and scan-matching constraints exist over that time interval. The robot trajectory $\boldsymbol{c}(t)$ is finally estimated by incrementally minimizing the error

$$E(\boldsymbol{c}\,(t-w{:}t)) = \sum_{<t_i,t_j>\in\mathcal{C}_O} \boldsymbol{\Theta}_O(\boldsymbol{c}_{i,j}) + \sum_{<t_i,t_j>\in\mathcal{C}_S} \boldsymbol{\Theta}_S(\boldsymbol{c}_{i,j}) \tag{1}$$

on the sliding window. This approach is flexible and allows registration of further error terms, e.g., loop closure constraints.

The global 3D map is the result of (i) projecting individual laser scans from their respective recording locations $\boldsymbol{c}(t_i)$ into a world reference frame and (ii) optionally applying point cloud post-processing filters, e.g., downsampling. For removing dynamic objects in the map, the system offers a probabilistic filtering based on octomaps.

The SLAM approach furthermore allows the reuse of previously recorded maps in subsequent sorties. The current approach for map merging aligns the robot's previous world reference frame with the current one at starting time and loads the previous map. The robot then continues mapping by constructing a new pose graph from its starting location. Both the loaded map and the updates are accessible to other robot modules, e.g., the path planner, giving rise to persistent use of multi-sortie information.

B. *Path planning on built maps*

The navigation module accepts as input both online registered point clouds and maps built in past sorties. When new sensory data is available and if substantial changes occurred in the map, the structure interpretation of the point cloud is updated. As a first step, the point cloud is filtered and *geometric features* such as normals and surface curvatures are computed. Then, segmentation is performed and clusters are labeled according to geometrical constraints applied to surface normal directions, mean curvatures and 3D-coordinates of points. This results in a classification of the environment in regions such as *walls*, *terrain*, *surmountable obstacles* and *stairs/ramps* [4, 5]. Traversability is then computed as a *cost function* taking into account the point cloud classification and the local geometric features [4, 5] (such as obstacle clearance, terrain roughness and point cloud density).

Path planning is performed both on global and local scales. Given a set of waypoints as input, the *global* path planner checks the existence of a traversable path joining them. Once a solution is found, a *local* path planner drives the robot towards the closest waypoint by continuously replanning a feasible path in a local neighbourhood in order to take into account possible dynamic changes in the environment. On both global and local scale, the connectivity of the traversable terrain is captured by using a sampling-based approach. In particular, a tree is expanded in the configuration space by using a randomized A* approach [4, 5].

III. INTEGRATED SCENARIO EXPERIMENTS

The full system was evaluated at the latest TJEx experiments where firemen end-users performed a search and rescue mission by teleoperating two TRADR UGVs. Amongst other sensors, these skid-steered vehicles are equipped with a 360° spherical camera and a rotating laser scanner as shown in Fig. 1, top-right.

An initial sortie was executed during the first mission day resulting in the map depicted in Fig. 1. On the second mission day, a second sortie was performed with a different robot, extending the map generated during the first sortie. The resulting merged map was displayed to the end-users in the command post through the TRADR OCU.

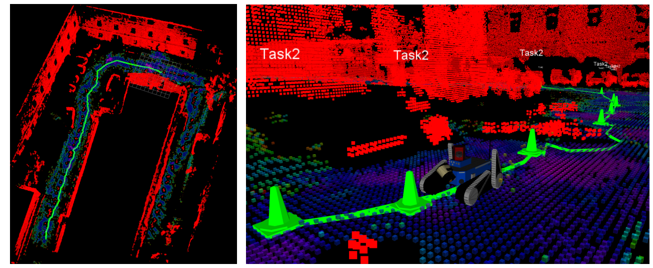

Figure 2: *Left*: Segmentation of the merged map into obstacles (red) and traversable regions (blue); a globally planned path (green line) is shown on the traversable region. *Right*: An example of planned path (green line) joining a set of waypoints (green traffic cones) selected by the end-user, directly on the traversability map.

During each mission, the end-users were able to identify points of interest and mark them as navigation waypoints on the traversability map (Fig. 2, left). Each set of selected waypoints was fed into a *task queue* managed by the global path-planner, which was always able to successfully compute a traversable path (Fig. 2, left). At execution time, the local path-planner and the trajectory control safely drove the vehicle along the planned paths (Fig. 2, right) by performing a continuous replanning in order to manage possible low-dynamic changes occurring in the environment. Autonomous waypoint inspection was successfully performed allowing end-users to detect victims and possible gas leaks.

IV. CONCLUSION

In this report we have shown the results of the mapping and path planning systems on the latest TJEx. A full map was obtained from different sorties by tele-operating the robots for exploration of the disaster area. This allowed to reduce the level of tele-operation in posterior sorties by automatically planning suitable paths on the built map for further inspection of interest points. Remarkably, the firemen were able to fully operate the robots by using the TRADR OCU which demonstrated the robustness and reliability of our 3D localization, mapping, and path planning systems. These results bring the goal of effective human-robot teaming closer to reality.

REFERENCES

[1] D. Tardioli, *et al.*, "Robot teams for intervention in confined and structured environments," *Journal of Field Robotics*, 2015.

[2] F. Pomerleau, F. Colas, R. Siegwart, and S. Magnenat, "Comparing icp variants on real-world data sets," *Autonomous Robots*, vol. 34, no. 3, pp. 133–148, 2013.

[3] G. Grisetti, R. Kümmerle, C. Stachniss, and W. Burgard, "A tutorial on graph-based slam," *Intelligent Transportation Systems Magazine, IEEE*, vol. 2, no. 4, pp. 31–43, 2010.

[4] G. Kruijff, , *et al.*, "Designing, developing, and deploying systems to support human–robot teams in disaster response," *Advanced Robotics*, vol. 28, no. 23, pp. 1547–1570, 2014.

[5] M. Menna, M. Gianni, F. Ferri, and F. Pirri, "Real-time autonomous 3d navigation for tracked vehicles in rescue environments," in *Proc. of the IEEE/RSJ Int. Conf. on Intelligent Robots and Systems*, 2014.

[6] M. Gianni, F. Ferri, M. Menna, and F. Pirri, "Adaptive robust three-dimensional trajectory tracking for actively articulated tracked vehicles," *Journal of Field Robotics*, pp. n/a–n/a, 2015. [Online]. Available: http://dx.doi.org/10.1002/rob.21584

[7] V. Kubelka, *et al.*, "Robust data fusion of multimodal sensory information for mobile robots," *Journal of Field Robotics*, vol. 32, no. 4, pp. 447–473, 2015.